SHEAR CAPACITY OF REINFORCED CONCRETE COLUMNS RETROFITTED WITH VERY FLEXIBLE FIBER REINFORCED POLYMER WITH VERY LOW YOUNG'S MODULUS

Hu Shaoqing* **Supervisor: Susumu KONO****
MEE08165

ABSTRACT

FRP with low Young's modulus (SoftFRP) was developed in the late 1990's and early 2000's. Polyketone fiber is a kind of new material of FRP with low Young's modulus and made from carbon monoxide and ethylene. And compared with aramid fiber, its material cost is lower. To investigate the improvement of shear strength of column wrapped with this kind of FRP sheets, four specimens among which one was unstrengthened and three specimens were wrapped by different amount of FRP sheets which provided the equivalent shear reinforcement ratio was 0.04%, 0.08% and 0.12% were tested. All specimens were tested under lateral reversal cyclic loading and a constant axial load. It is found that the shear strength of the RC column effectively increased with strengthening FRP sheet. And it prevents the sudden brittle fracture of the column because of the confinement of FRP sheets with large deformation capacity. The shear resistance of the FRP sheet becomes effective after the yield of shear reinforcement, and the strain of FRP sheet becomes large. The shear contribution of the FRP sheets could be explained by truss-arch shear resisting mechanism.

Keywords: FRP with low Young's modulus (SoftFRP), shear strength, truss-arch mechanism.

1. INTRODUCTION

FRP with low Young's modulus (SoftFRP) was developed in the late 1990's and early 2000's. It was made from relatively economic material like polyacetar [Iihoshi 2005] or polyester [Igarashi 2000]. Compared to CFRP, FRP with low young's modulus has low cost, easy construction, few dust and noise. So it is applicable to be used as a retrofitting material [Kono 2008]. Polyketone fiber is a kind of new material of FRP with low Young's modulus and made from carbon monoxide and ethylene. And compared with aramid fiber, its material cost is relative low. To investigate the improvement of shear strength of column wrapped with polyketone fiber sheets, four specimens of columns, one is un-retrofitted and three other specimens retrofitted, were tested under constant axial load and lateral cyclic load.

2. TEST SETUP

2.1. Specimen

The specimen was a vertical column fixed at the top and bottom, as shown in Figure 1. The stubs of top and bottom are strong enough as fixed ends for the column. The column had a rectangular

* Institute of Engineering Mechanics (IEM), China Earthquake Administration (CEA) , China
** Assoc. Prof., Department of Architecture and Architectural Engineering, Kyoto University, Japan

cross-section 400mm×400mm and a total length of 1200mm. All specimens had the same reinforcement detailing. The steel reinforcement was twelve D16 (SD 295A) for longitudinal reinforcement and D6 (SD 295A) for transverse reinforcement at 100mm spacing. The shear (span/depth) ratio, 1.5 and the axial force ratio, 0.3 were adopted in the specimen design.

For the strengthened test specimens, the unidirectional FRP sheet strips made from polyketone were impregnated with epoxy resin and wrapped around the column with different spaces. And the equivalent reinforcement ratios of specimen D15F04, D15F08 and D15F12 provided by FRP were 0.04%, 0.08% and 0.12%, respectively. The width of the FRP strip was 75mm with the thickness of 0.333mm.

The specimen parameters are listed in the Table 1. For Specimens D15F00 and D15F12, the compressive strength is 18.8MPa. And for Specimens D15F04 and D15F08, the compressive strength is 14.6MPa. The material properties of steel and FRP material are shown in Table 2.

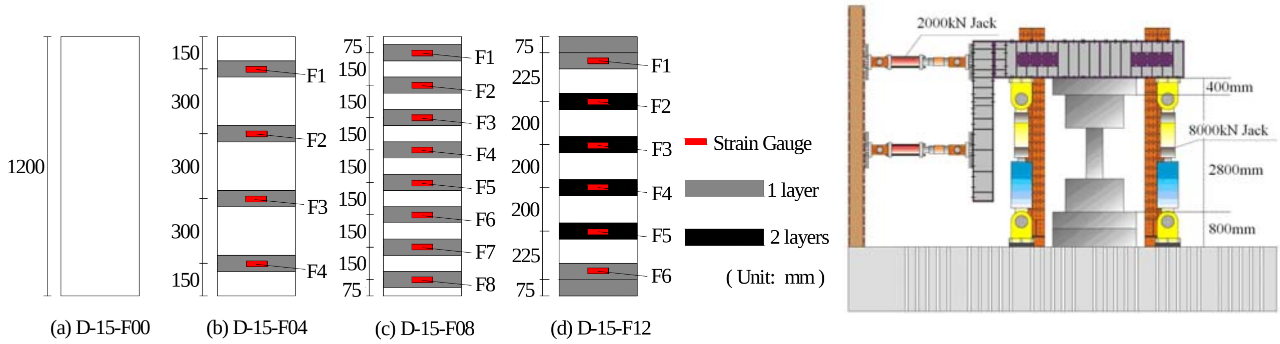

Figure.1 Four specimens and strain gauges on FRP sheet

Table 1 Details of Specimens

Specimen	Compressive strength of concrete Fc (MPa)	Axial force ratio	Concrete Young's modulus (MPa)	FRP sheets (75mm of width)	The equivalent reinforcement ratio of FRP
D-15-F00	18.8	0.3	2275	No	0%
D-15-F04	14.6	0.3	1942	4 strips×1 layer	0.04%
D-15-F08	14.6	0.3	1942	8 strips×1 layer	0.08%
D-15-F12	18.8	0.3	2275	6 strips×2 layers	0.12%

Table 2 Material properties of steel bar and FRP sheets

Materials	Type	Yield Strength (MPa)	Tensile Strength (MPa)	Young's modulus (GPa)	Yield strain (%)
Steel	D6	407	520	173	0.235
	D16	366	527	185	0.198
FRP	Polyketon fiber	1709	-	37.6	4.54

2.2. Loading and Measuring System

Cyclic reversed horizontal loads were statically applied to the specimens by two 2000kN hydraulic jacks in both positive and negative directions. During the cyclic horizontal loading, vertical axial loads were also applied by two 8000kN hydraulic jacks. The vertical axial load levels were determined in accordance with the axial force ratio designed to be 0.3 which was first applied and then maintained constant during the test. Loading was mainly controlled by measured displacement in terms of the member drift angle which was computed by averaging lateral displacements measured at north and south ends of column over the effective length of 1200mm. The first cycle of loading was performed up to 50kN with load controlled. Subsequently two cycles of repeated loading were applied for each drift angle: ±0.1%, ±0.25%, ±0.5%, ±0.75%, ±1.0%, ±2.0%, ±4.0%, ±6.0% by using displacement controlled. The test was terminated when the specimen could not sustain the axial force.

Two displacement transducers were attached to the central section of the top stub and the bottom stub separately to measure the relative displacement of the specimen. The strains of the longitudinal reinforcement, shear reinforcement and FRP sheets in the test region were measured by strain gauges attached on the surface of the steel bars and FRP sheets, respectively.

3. EXPERIMENTAL RESULT

3.1. Test Observation

Figure 2 presented damage of specimens at the drift angle R=4.0%. Shear crack occurred at drift angle R=0.50%, R=-0.375%, R=0.25%, R=0.25% for Specimen D15F00, Specimen D15F04, Specimen D15F08, Specimen D15F12, respectively. With the increase of drift angle, more shear cracks formed and the width of shear cracks increased. For the retrofitted specimens, it was observed that the FRP sheets and concrete all dilated. For Specimen D15F00, at the first loading cycle at R=4.0%, cover spalling in the middle of column was observed and the longitudinal bar buckled, then the specimen could not sustain the axial force. For Specimens D15F04 at the first loading cycle R=4.0%, Specimen D15F08 at second loading cycle R=4.0%, Specimen D15F12 at first loading cycle R=6.0%, and FRP sheets fractured, cover spalled off and the longitudinal bar buckled then the axial force could not sustained.

(a) D-15-F00 (b) D-15-F04 (c) D-15-F08 (d) D-15-F12

Figure 2 Damage of specimens (at the drift angel R=4.0%)

The maximum load capacity and drift angle at the positive direction and negative direction and the initial stiffness are presented in Table 3. Compared to Specimen D15F00, Specimen D15F12 increased the ultimate capacity Q_{max} from 352.0kN to 413.1kN. And the drift angle corresponding to the maximum lateral load changed from 0.488% to 0.758%. Compared to Specimen D15F04, Specimen D15F08 increased the ultimate capacity Q_{max} by 11.5%. The effect retrofitted by FRP on improving the ultimate capacity is rather obvious The difference of initial stiffness of four specimens is small. So it can be considered that the FRP did not affect the initial stiffness but the shear strength.

From the envelope of lateral load-drift angle curves, the degradation of shear strength of Specimens D15F08 and D15F12 is gentler than that of Specimen D15F00. It may be said that the confinement of FRP increased the ductility of column.

Table 3 Summary of test results

Specimen	Initial stiffness (10^5 kN/rad)	Maximum lateral load capacity			
		Positive		Negative	
		R (%)	Q_{max} (kN)	R (%)	Q_{max} (kN)
D15F00	1.70	0.488	352.0	-0.481	-359.4
D15F12	1.82	0.758	413.1	-0.498	-361.4
D15F04	1.74	0.475	334.3	-0.498	-311.2
D15F08	1.75	0.513	372.9	-0.401	-330.8

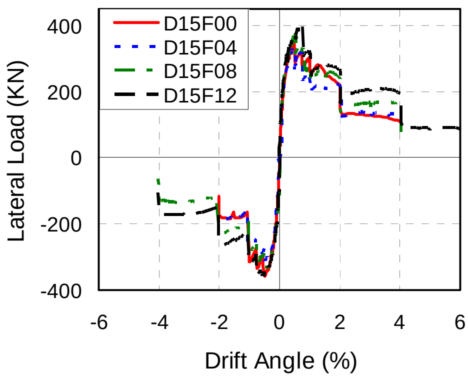

Figure 3 Envelop of the lateral load-drift angle relation

3.2. Strain Development in FRP Sheets

The shear contribution provided by the wrapped FRP sheet was studied in detail by the strain gauges pasted on it. The strain distributions of the FRP sheet are shown in Figure 4. It was observed that the strain of the FRP sheet was very small before the shear cracks occurred and began to increase very quickly after shear cracking. And the strain of middle FRP strips is larger than that of end FRP strips. For D-15-F04 and D-15-F08 at the drift angle R=0.5%, and for D-15-F12 at the drift angle R=0.75%, the strain increased dramatically. It agrees with the yield of shear reinforcement. And the strain of FRP sheet at the maximum lateral load did not attain its fracture strain.

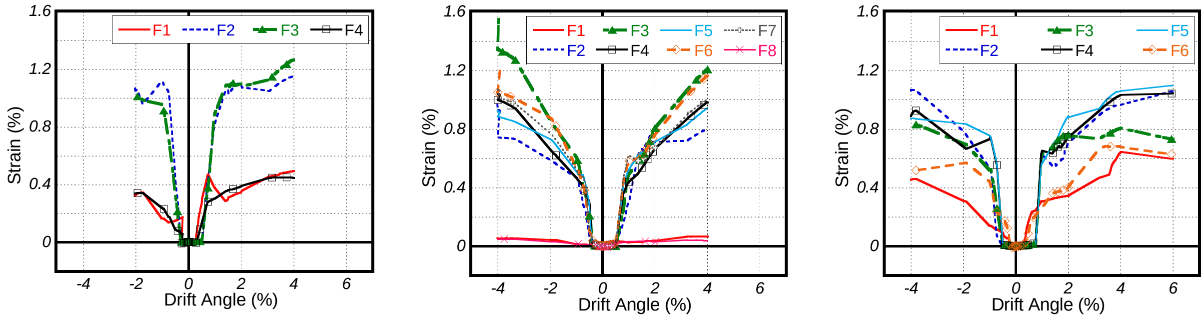

(a) D-15-F04 (b) D-15-F08 (c) D-15-F12

Figure 4 Strain developments in FRP Sheets

4. ANALYTICAL SIMULATION

4.1. Shear Strength Calculation Based on FRP Specifications

According to the design and construction guideline of continuous fiber reinforced concrete [AIJ 2001], the ultimate shear strength of column and beam retrofitted by continuous fiber sheet can be calculated by Eq. (1).

$$Q_{su} = b\, j_t \sum (p_w \sigma_w) \cot\phi + \tan\theta (1-\beta) bDv\sigma_B / 2 \tag{1}$$

$$\sum (p_w \sigma_w) = p_{ws}\sigma_{wys} + p_{wf} E_{fd} \varepsilon_{fd}$$

p_{ws}, σ_{wys} are the shear reinforcement ratio and the yield strength of shear reinforcement; p_{wf} : the equivalent shear reinforcement ratio of continuous fiber sheet with effective thickness t_{wf} ; $p_{wf} = 2t_{wf}/b$. E_{fd} : The Young's Modulus of continuous fiber sheet; ε_{fd} : Effective strain of continuous fiber sheet.

The effective strain of continuous fiber sheet can be calculated by Eq. (2). And the value $E_{fd}\varepsilon_{fd}$ can not exceed 2/3 of the tensile strength σ_f of continuous fiber sheet.

$$\varepsilon_{fd} = 0.009 - 0.0002 \frac{p_{wf} E_{fd}}{\sigma_B} \tag{2}$$

If $\frac{p_{wf} E_{fd}}{\sigma_B}$ >20, then ε_{fd} =0.005;

The effective factor of concrete is given in Eq.(3)

$$v = 0.7 - \sigma_B / 200 \tag{3}$$

For Specimen D15F00, the shear strength calculated by using the effective factor of concrete compressive strength shown in Eq.(3) is lower than the experiment value 352kN. The objective of the experiment is to find the relation between the amount of retrofitting material and the increase of shear capacity. So for Specimen D15F00, the effective factor of concrete compressive strength was recalculated according to the calculated shear strength equaling to the experiment data. And the following Eq.(4) was used. The calculated shear strength is consistent with the experiment value according to the modified effective compressive strength of concrete (Table 4).

$$\nu = 1.0 - \sigma_B / 200 \tag{4}$$

4.2. Shear Resisting Mechanism of Column Retrofitted by FRP Sheets

To further understand shear resisting mechanism of column retrofitted by FRP sheets, the shear resistant forces of shear reinforcement and FRP are calculated according to the strain obtained from experiment respectively. Figure 5 presented the total shear force measured during test versus calculated shear force carried by the stirrups. For four specimens, there is no quite difference until the drift angle R=0.25%. After 0.25%, shear force carried by stirrups for Specimen D15F00 is lower than that of Specimen D15F12 at the same drift angle. And the shear force carried by stirrups of Specimen D15F04 is larger than that of Specimen D15F08. Figure 6 showed the calculated shear force carried by FRP sheets for Specimen D15F04, D15F08 and D15F12. For three retrofitted specimens the calculated shear force carried by FRP sheets is almost equal to 0.0kN until drift angle R=0.25%. After 0.25%, the shear force carried by FRP sheets increased quickly for Specimen D15F04 and Specimen D15F12, but increased quite slowly for Specimen D15F08.

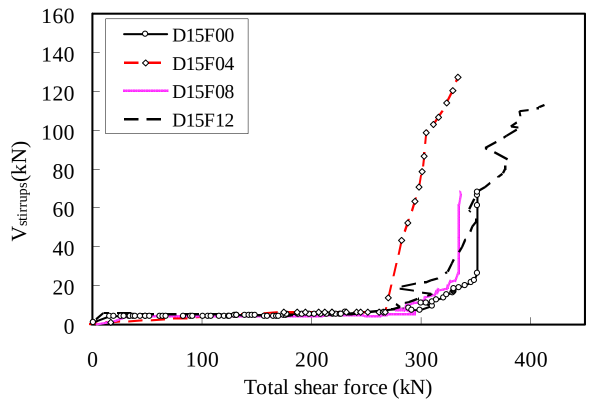

Figure 5 Shear force carried by stirrups

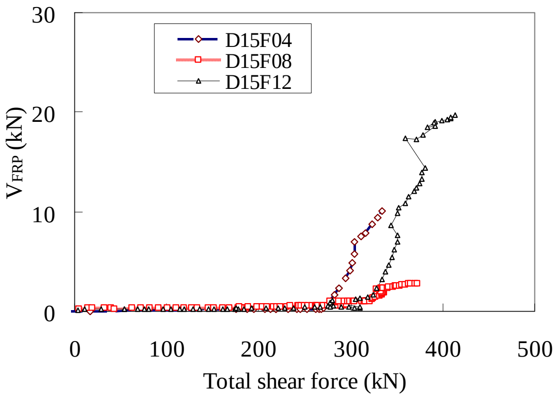

Figure 6 Shear force carried by FRP sheets

4.3. Analytical Results Compared to Experimental Results.

Table 4 presented the calculated shear strength, calculated flexural strength and test results. The ultimate flexural strength of column can be accurately predicted based on fiber model using the strain- or stress-compatibility theories.

Shear failures occur when the shear capacity of column exceeds prior to the load level reaching the flexural strength. From this point, it can be said the failure mode of Specimen D15F00 and D15F04 is shear failure. Shear strength calculated by design equation using the effective factor Eq.(3) is lower than experimental results. And the ratios of the experimental figures to the calculated figures are 1.28 and 1.18 separately. However, for the design equation using modified effective factor, ν the shear strength agreed well on the experiment value. So it maybe said that the design equation underestimate the ultimate shear strength.

The load level reached the flexural strength at first for the Specimen D15F12 and its behavior flexural failure mode. The failure mode of Specimen D15F08 is flexural failure due to the longitudinal bar yield when the lateral load reaches the maximum load. Shear strength calculated by design equation using the effective factor Eq.(3) is underestimated. And the ratios of the experimental figures to the calculated figures are 1.19 and 1.10 separately.

So if using the design equation to get the ultimate shear strength, some modification should be considered.

Table 4 Calculated results compared to test results

Specimens	Calculated Results(kN)				Flexural		Test Result (kN)		Failure mode
	ν Eq.(3)		ν Eq.(4)		Strength(kN)		Positive	Negative	
D15F00	277.4	(1.28)	350.6	(1.00)	384.9	(0.91)	352.0	-359.4	Shear
D15F12	352.2	(1.10)	425.5	(0.97)	384.9	(1.07)	413.1	-361.4	Flexural
D15F04	274.0	(1.18)	330.9	(1.01)	340.2	(0.98)	334.3	-311.2	Shear
D15F08	298.6	(1.19)	355.5	(1.05)	340.2	(1.09)	372.9	-334.8	Flexural

5. CONCLUSIONS

Polyketone fiber is a kind of new material of FRP with low Young's modulus and made from carbon monoxide and ethylene. This paper analyzes the test results of four specimens among which three specimens wrapped with FRP strips and calculated the shear force contributed by FRP strips to understand how it worked after the shear reinforcement yield. And the following results were obtained.

The strains in FRP sheets were higher than those in shear reinforcement after the yield of shear reinforcement. The shear resistance of the FRP sheet becomes effective after the yield of shear reinforcement. It can be said that the confining action of column distributed moved from the shear reinforcement to the FRP sheets. It prevents the sudden brittle fracture of the column because of the confinement of FRP sheets with large deformation capacity.

For Specimens D15F00 and D15F04, shear failure occurred before bending yield. Shear strength calculated by design equation using the effective factor Eq.(3) is lower than experiment results. However, the shear strength using modified effective factor, ν agreed well on the experiment value. So it maybe said that the design equation underestimate the ultimate shear strength. Specimens D15F08 and D15F12 are flexural yielding precedence. It is observed that the ultimate shear strength calculation based on FRP specifications is underestimated. It means that the assessment is made in a safe side. So the ultimate shear strength calculation based on FRP specifications is used, some modification should be considered.

ACKNOWLEDGEMENT

I would like to express my sincere gratitude to Assoc. Prof. S. KONO and the advisor Dr. T. MUKAI for their continuous support, valuable suggestion and guidance during my study.

REFERENCE

Architectural Institute of Japan (2001), Design and Construction Guideline of Continuous Fiber Reinforced Concrete, AIJ, (In Japanese), pp.289

Igarashi, S., 2000, Proceedings of the third Japan-Turkey workshop on earthquake engineering, February 22, Istanbul.

Iihoshi, C., Fukuyama, H. and Tanaka, H., 2005, International Symposium on Earthquake Engineering Commemorating Tenth Anniversary of the 1995 Kobe, Kobe/Awaji, Japan.

James G. MacGregor, James K. Wight, 2005, Reinforced Concrete Mechanics and Design (Fourth Edition), Prentice Hall

Kono, S., Doi, M., Lee, J., Tanaka, H., 2008. 14th World Conference on Earthquake Engineering.

Michael P.Collins, 1991, Denis Mitchell, Prestressed concrete structure, Prentice-Hall, Inc.

Website: http://findarticles.com/p/articles/mi_qa5358/is_200503/ai_n21369170/.